

Fluoride and calcium-phosphate coated sponges of the magnesium alloy AX30 as bone grafts: a comparative study in rabbits

Mareike Lalk · Janin Reifenrath · Nina Angrisani ·
Alexandr Bondarenko · Jan-Marten Seitz ·
Peter P. Mueller · Andrea Meyer-Lindenberg

Received: 18 July 2012 / Accepted: 6 November 2012 / Published online: 17 November 2012
© Springer Science+Business Media New York 2012

Abstract Biocompatibility and degradation of magnesium sponges (alloy AX30) with a fluoride (MgF_2 sponge, $n = 24$, porosity $63 \pm 6 \%$, pore size $394 \pm 26 \mu\text{m}$) and with a fluoride and additional calcium-phosphate coating (CaP sponge, $n = 24$, porosity $6 \pm 4 \%$, pore size $109 \pm 37 \mu\text{m}$) were evaluated over 6, 12 and 24 weeks in rabbit femurs. Empty drill holes ($n = 12$) served as controls. Clinical and radiological examinations, in vivo and ex vivo μ -computed tomographies and histological examinations were performed. Clinically both sponge types were tolerated well. Radiographs and XtremeCT evaluations showed bone changes comparable to controls and mild gas formation. The μCT80 depicted a higher and more inhomogeneous degradation of the CaP sponges. Histomorphometrically, the

MgF_2 sponges resulted in the highest bone and osteoid fractions and were integrated superiorly into the bone. Histologically, the CaP sponges showed more inflammation and lower vascularization. MgF_2 sponges turned out to be better biocompatible and promising, biodegradable bone replacements.

1 Introduction

The bridging of critical size bone defects, which would overburden normal bone regeneration and result in non-unions [1–3], is still a considerable challenge for orthopedic surgeons [4]. The use of autografts is deemed the “gold standard” (method of first-choice) since they convey osteogenic cells as well as endogenous growth factors, and exhibit a high incorporation rate with early revascularization [4–9]. However, one can fault the limited availability, elevated fracture rates and donor site morbidity [5, 10–12].

In recent years, intensive research has been undertaken on the development of synthetic bone replacement materials. Ideally, these replacements should be porous, highly biocompatible, three dimensional and with sufficient mechanical strength [2, 8, 13]. Besides porous calcium-phosphate compounds, ceramics and polymers [1, 14, 15], metallic sponges and or foams made of titanium, iron, aluminum and magnesium alloys have attracted great interest owing to their superior mechanical properties [16–19]. Of these alloys, only the titanium alloys are routinely employed as monolithic non-porous (solid) and porous implants in bone surgery [20, 21]. However, even these alloys are not biologically inert and can provoke metallosis with massive accumulations of macrophages and T-cells including occasional allergic reactions [20, 22]. Hitherto, no in vivo bone biocompatibility studies have been

M. Lalk (✉) · J. Reifenrath · N. Angrisani
Small Animal Clinic, University of Veterinary Medicine
Hannover, Bünteweg 9, 30559 Hannover, Germany
e-mail: mareike.lalk@tiho-hannover.de

A. Bondarenko
Department of Pathology, Dnipropetrovs'k State Medical
Academy, Street Zhovtneva Ploshcha 14,
Dnipropetrovs'k 49005, Ukraine

J.-M. Seitz
Institute of Materials Science, Leibniz Universität Hannover,
An der Universität 2, 30823 Garbsen, Germany

P. P. Mueller
Department of Gene Regulation and Differentiation,
Helmholtz Centre for Infection Research, Inhoffenstrasse 7,
38124 Braunschweig, Germany

A. Meyer-Lindenberg
Clinic for Small Animal Surgery and Reproduction, Centre
of Clinical Veterinary Medicine, Faculty of Veterinary
Medicine, Ludwig Maximilian University Munich,
Veterinärstraße 13, 80539 Munich, Germany

published in the accessible literature on biodegradable iron foam alloys. However, intraperitoneal injections of iron-dextrane reduced the activity of bone formation in rats [23]. Depending on the alloy composition, solid biodegradable magnesium implants appear promising due to high stiffness to weight ratios [24] and good biocompatibility without allergenic potential [25] together with high rate of bone regeneration associated with slow implant degradation [26–30].

However, in earlier *in vivo* studies, casted, uncoated AZ91 sponges with a pore size of 10–1,000 μm degraded too rapidly over 12 and 24 weeks in a rabbit model [31]. The alloy AX30 appears to be better suited since, in comparison with other magnesium alloys, extruded cylindrical implants (2.5 \times 25 mm) made of AX30 exhibit the lowest weight reduction after 6 months implantation in the rabbit tibia [29]. Here, as an extruded solid pin with a corrosion rate of 0.11 mm^2/y , the alloy degraded homogeneously over a long time period without obvious changes of the implant geometry and its mechanical strength is similar to that of MgCa0.8 [29, 32]. In addition to this, the corrosion resistance of magnesium alloys can be increased by means of a coating [26, 33]. Up until now, the alloy AX30 has been investigated as a bioglass coated sponge within the scope of a pilot study [34]. These sponges degraded comparatively more slowly but still too rapidly for bone ingrowth. Fluoride coating was applied to different implants by several authors [27, 33, 35]. They could show that fluoride coating represents an alternative by which the pure magnesium, MgCa0.8 and LAE442 implants corroded more slowly and by which it was possible to achieve direct implant bone contact [27, 33, 35]. Additionally, other groups could show that the coatings could lead to a better filling of the sponge since augmented osteoid in the bone is formed by means of the systemic and localized administration of fluoride [36–38]. On the other hand, bioactive coatings of calcium-phosphate compounds are frequently considered which, apart from the degradation, could also improve the surface bioactivity. In addition, in particular during early implantation stages, it could accelerate bone formation and maturation at the implant-tissue-interface by means of promoting osteoblast proliferation [26, 30, 39]. The combination of both coating materials in the form of MgF_2 interlayers turned out to be especially advantageous due to improved coating implant bonding [26].

Thus in the current study, the biocompatibility, the degradation and bone ingrowth behavior of AX30 magnesium alloy sponges with a solely fluoride coating were to be compared to that of AX30 magnesium alloy sponges with a fluoride and additional calcium phosphate coating.

2 Materials and methods

2.1 Implants

2.1.1 Sponge preparation

Cylindrical sponges (length 4 mm, \varnothing 3 mm; $n = 48$) were produced of the magnesium alloy AX30 (3 wt % aluminum, ≤ 1 wt % calcium) via die casting processes [24].

In the same way as for solid magnesium implants the MgF_2 coating was carried out by means of boiling in sodium hydroxide (NaOH, Merck, Darmstadt, Germany, 200 g/l, 120 min) at 107 °C, washing up in distilled water and placing into hydrofluoric acid (AppliChem, Darmstadt, Germany, 40 %, 96 h) [40]. The final step was performed with vacuum in an evacuable desiccator to safeguard the penetration of acid into the pores. Subsequently the sponges were dipped into distilled water and ethanol for 3 min each. For the thorough removal of the chemicals required for the coating the sponges were fixed separately in a tube between two lattice structures and rinsed three times in a vacuum with distilled water and ethanol. To ensure a total elimination of the flush media and to prevent the beginning of corrosion ahead of time the sponges (MgF_2 sponges) were blown through with compressed air.

For the calcium-phosphate coating a viscous suspension of a saturated di-ammonium-phosphate (Merck, Darmstadt, Germany) solution and tri-calcium-phosphate powder (Sigma–Aldrich, Seelze, Germany) was produced. This paste was pressed into the pores of previously fluoride coated sponges via centrifugal force and vacuum (5 min) within an Eppendorf concentrator 5301 (Eppendorf, Hamburg, Germany). After manual remove of excess coating material the sponges were dipped into a further suspension made of a saturated di-potassium-hydrogen-phosphate (Merck, Darmstadt, Germany) solution and a calcium hydroxide powder (Merck, Darmstadt, Germany) to alkalinize the magnesium surface. In a drying cabinet (65 °C, 15–20 h) the coating of the sponges (CaP sponges) hardened.

2.1.2 SEM/EDX

In order to check the regularity and the element composition of the coatings as described by Thomann et al. one sponge per coating type was investigated exemplarily in a scanning electron microscope ((SEM) LEO 1455VP, Zeiss, Oberkochen, Germany) and by energy dispersive X-ray spectroscopy ((EDX), EDAX Genesis, EDAX, Mahwah, USA) [27].

2.1.3 μ -Computed tomography

For an exact characterization of the basic implant properties six sponges of each coating type were scanned in a high-resolution μ -computed tomography (μ CT80, Scanco Medical, Zurich, Switzerland; 55 kVp, 72 μ A, voxelsize 10 μ m, integration time 1,000 ms). After contouring and determining of threshold values for obviously different shaded regions (gauss sigma 1.0, gauss support 2.0; threshold values: CaP sponge coating 319–1,000, sponge 172–318, hypodense material 99–171 and air –1,000–98) the analysis was performed using a true 3D evaluation software (μ CT evaluation program V6.0, Scanco Medical, Zurich, Switzerland) for 3D and local 3D calculation. Prior to implantation all sponges were sterilized separately in sterilization bags (Krauth und Timmermann, Isernhagen, Germany) by exposure to gamma radiation (BBF-Serilisationservice GmbH, Kernen, Germany, 25 kGy, 8 h) according to DIN EN ISO 11137:2006.

2.2 Animal model

In accordance with §8 of the animal protection law the animal experiments were approved by the Federal Office for Consumer Protection and Food Safety with the reference number 33.9-42502-04-08/1492. 30 adult female New Zealand white rabbits (Charles River, Sulzfeld, Germany, weight: 3.47 ± 0.46 kg) were randomly divided into three time groups of 6, 12 and 24 weeks ($n = 10$ rabbits), respectively. Three experimental groups (MgF₂ sponges ($n = 8$), CaP sponges ($n = 8$) and empty drill holes ($n = 4$)) were investigated in each time group. One sponge, was implanted into the cancellous part of the left and right greater trochanter of the femur of the rabbits, respectively. In four animals per time group one trochanter got a sponge and the contralateral trochanter underwent the same operation procedure, but remained empty and served as a control (in the following referred to as “empty”). Empty drill holes were chosen as control to differentiate between effects due to the operation procedure or to the sponges and to estimate the dimension of defect healing support by the sponges. Operation and post-operative treatment were carried out as described by Lalk et al. [34]. Briefly, during the operation in general anesthesia a lateral access to the greater trochanter was accomplished through an incision of 3 cm into skin and fascia and temporary displacement of muscles. Then a hole (3 × 5 mm) was drilled into the middle of the trochanter in direction to the femoral head and one sponge was inserted into the cancellous part, so that it lay just 1 mm under the bone surface (Fig. 1). Afterwards the wound was sutured multilayered with SAFIL[®] violet 4/0 (B. Braun Melsungen AG, Melsungen, Germany). During the following 10 days the rabbits

received analgetic and antibiotic drugs. The animals were housed in standard cages (4,250 cm², EC3, Scanbur-BK, Karlslunde, Denmark) and fed daily with 100 g Altromin 2,123 pellets (Altromin Spezialfutter GmbH und Co KG, Lage, Germany) and accordingly hay and water ad libitum.

2.3 Postoperative investigation period

2.3.1 Clinical examination

A general and an orthopedic examination of the rabbits were performed daily. Special attention was paid to redness, swelling, emphysema, firm or soft peripheral augmentations beside the drill hole, pain, lameness and infection. For analysis, the parameters were assessed descriptively.

2.3.2 Radiological examination

Digital X-ray images (Practix 160, Philips, Hamburg, Germany, 48 kV, 6.3 mAs) of all animals were recorded weekly in HD-position. For evaluation the program dicomPACS[®] vet (Version 5.2.4; Oehm und Rehbein GmbH, Rostock, Germany) was used. The parameter gas outside the bone was assessed descriptively, while the parameters periosteal bone formation in the drill hole periphery (size in mm) and radio-opaque structures in the adjoining muscle tissue (number and accordingly mm) were analyzed using the semiquantitative scoring system

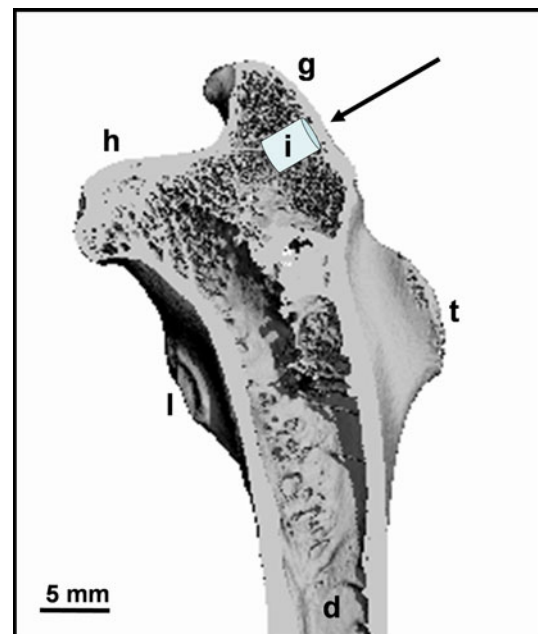


Fig. 1 Implant site in a rabbit femur (front view; *i* implant, *h* femur head, *g* greater trochanter, *l* lesser trochanter, *t* third trochanter, *d* femur diaphysis, arrow drilling direction)

described by Lalk et al. [34]. Therefore score values from 0 (not existing) to 2 (clear alteration) were given. The values of the individual animals for each investigation time were added to a total score, which was used as base for the group's arithmetic mean value at the respective investigation time.

2.3.3 In vivo μ -computed tomography

With the XtremeCT (Scanco Medical, Zurich, Switzerland, 60 kVp, 901 μ A, voxelsize 41 μ m, integration time 200 ms) the rabbits were scanned in general anesthesia (introduction with ketamine-hydrochloride (10 mg/kg, Ketamin 10 %, CP-Pharma Partner GmbH, Burgdorf, Germany) and medetomidine (0.125 mg/kg, Domitor[®], Pfizer Pharma GmbH, Berlin, Germany), maintenance with isoflurane (2.5–3.5 vol % in oxygen mixture, Isoba[®], Essex Pharma GmbH, Munich, Germany)) direct postoperatively, biweekly up to the 8th week and every 4 weeks in the following. For analysis, five standardized slices in the amount of 20, 40, 50, 60 and 80 % of the remaining, degrading implant (Fig. 2a) were observed using a semi-quantitative scoring system described by Lalk et al. [34]. Subsequently one score value for the whole scan was given for each parameter. The established scoring system included the parameters gas in- and out-side the bone (characteristic), periosteal bone formation in the drill hole periphery (size in mm), bone like structures in the adjoining muscle (number or mm) as well as the integration of the sponges into the bone (characteristic). The scoring system ranged from 0 = positive or physiological to 2 = negative or clearly altered. Furthermore, the sponge or defect position (score 0 = completely in cancellous bone to score 2 = reaching into medullary cavity) was assessed in the first scan [34]. For each experimental group and each parameter minimum, median and maximum of all score values given a certain time were calculated.

2.4 Postmortal examinations

2.4.1 Ex vivo μ -computed tomography

At the end of each investigation period the animals were euthanized with ketamine-hydrochloride (20 mg/kg, Ketamin 10 %, CP-Pharma Partner GmbH, Burgdorf, Germany) and xylazine-hydrochloride (5 mg/kg, Xylazin 2 % Bernburg, Serumwerk Bernburg AG, Bernburg, Germany), followed by an intracardial application of pentobarbital (912 mg/animal, Narkodorm[®], CP-Pharma Partner GmbH, Burgdorf, Germany). Both femurs were explanted and the greater trochanters were separated with a diamond band saw (Exakt 310, Exakt, Norderstedt, Germany). Furthermore, the bone sponge compounds, which were fixed in a 4 % formalin solution and uprightly aligned in a polypropylene tube (16.5 mm ϕ , Sarstedt AG & Co, Nümbrecht, Germany) by foam material, were scanned in the μ CT80 with the same adjustment as the sponges before implantation. Initially a two-dimensional analysis was done in the same way as in the in vivo μ CT with five standardized slices (Fig. 2a). A semi-quantitative scoring system established by Lalk et al. [34] was used and one score value per parameter for the whole scan was given. The scoring system included the parameters periosteal bone formation in the drill hole periphery (size in mm), integration of the sponge into the bone (characteristic), structure of the surrounding cancellous bone (characteristic), closing of the drill hole (characteristic) and sponge shape (characteristic). For the empty drill holes the parameters integration and sponge shape were excluded. The constitution 0 for positive or physiological to 2 for clearly altered attributes was maintained. Furthermore box plots of the collected score values were made. Finally the remaining drill hole width in the cortical bone was measured for each case in the slice with the widest range as distance (mm). For an additional three-dimensional analysis the

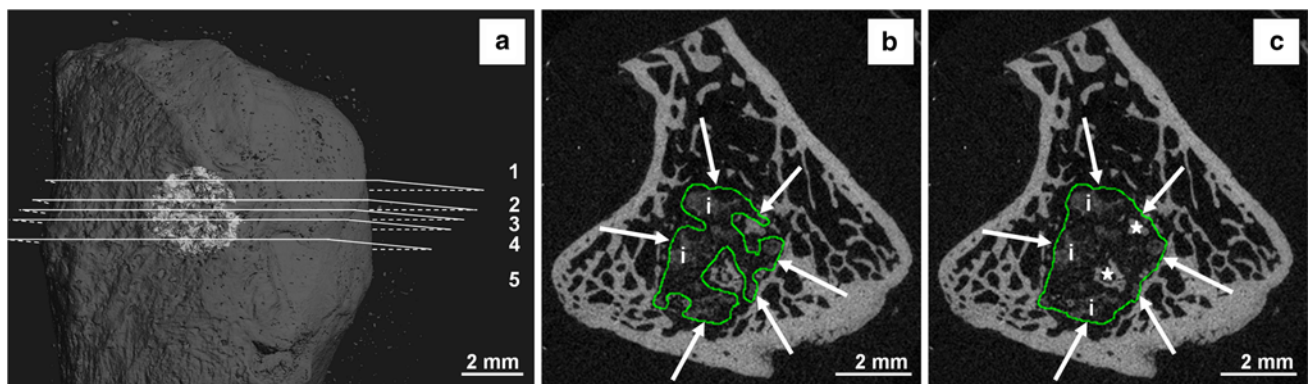


Fig. 2 MgF₂ sponge in the greater trochanter: 3D reconstruction of a μ CT80 scan with lines 1–5 according to the evaluated slices at 20, 40, 50, 60 and 80 % (a), 2D slices of a with an exact contour of a MgF₂

sponge (b) and an extended contour including the bone like fractions inside the sponge (c); the *arrows* show the contour, *i* implant, *asterisk* bone like fraction

sponge was differed visually from the bone within implant carrying trochanters using the parameters structure, shape, position and connection to the outer bone and accordingly contoured accurately in each slice (Fig. 2b). Using the same thresholds as for the sponge characterization the remaining volume, surface (inner and outer area of the sponge including the pores) and density of sponges and calcium-phosphate coating were calculated (μ CT evaluation program V6.0; Scanco Medical, Zurich, Switzerland). For evaluation of bone like fractions inside the sponge pores or sponge remnants an extended contour based on the exact sponge contour was made via direct connection of all adjacent outer sponge parts (Fig. 2c) and a new calculation was performed using the previous threshold. The values obtained were related to the basic values. Moreover, the arithmetic mean with standard deviation was calculated of the metric data collected in the ex vivo μ CT evaluation.

2.4.2 Histology

After at least 10 days formalin fixation the bone-sponge-compounds were embedded in 2-hydroxyethyl-methacrylate (Technovit[®] 7200 VLC; Heraeus Kulzer GmbH, Wehrheim, Germany) for histological examinations. Subsequently slices of ~50 μ m [32, 41] were produced based on the cutting and grinding technique according to Donath [42]. One centrally located cross section of each animal was subjected to a Toluidin blue staining (0.1 % Toluidin blue O, Chroma, Münster, Germany) as general staining technique [43]. For a standardized analyzation of the stained slices a circle of 4 mm diameter around the implant or the defect [44] was designated using the Axio Imager Z1 (Carl Zeiss MicroImaging GmbH, Göttingen, Germany). Within this circle the tissue reactions were evaluated by two independent experts through a semiquantitative (magnification 400-fold)

and -qualitative (magnification 100-fold) scoring system (Table 1) modified according to Jansen et al. [45]. Thereby giant cells and vessels in the whole area and bone reactions in three different areas, the bone located outside the implant, the bone-implant-interface and the interstitium as area inside the sponge, were investigated. Box plots were compiled of the collected data. Additionally, photos of the slices were taken at 100-fold magnification and the areas of osteoid (O.Ar) and mineralized bone (Md.Ar) inside the circle were contoured and calculated with the freeware program ImageJ (Version 2006.02.01). Furthermore, these areas were put in relation to the total area of the circle (O.Ar/Tt.Ar and Md.Ar/Tt.Ar), the osteoid fraction of the bone matrix, comprising osteoid and mineralized bone, was determined (O.Ar/B.Ar) and the arithmetic mean with standard deviation was calculated. The used terms and abbreviations correspond to the nomenclature recognized by the American Society of Bone and Mineral Research (ASBMR) [46].

Additionally, for each experimental and time group, except for the 24 weeks control group, one part of the musculus gluteus superficialis, which was located close to the insertion and included a firm, radio-opaque structure, was examined to distinguish between mineralized depositions and bone tissue. For that purpose the samples were decalcified in a 10 % ethylene-di-amine tetraacetic acid solution (EDTA-Dinatriumsalz-Dihydrat, AppliChem, Darmstadt, Germany, pH 7.4, 4 °C, 14 day) with daily solution change. Finally paraffin slices of 2–3 μ m were produced in a way described by Lalk et al. [34], stained with haematoxylin and eosin and evaluated descriptively.

2.5 Statistics

Statistical analyses were done with the programs Microsoft Office Excel[®], Version 2003 (Microsoft Cooperation,

Table 1 Scoring system for the histological evaluation of the bone sponge compound cross sections—evaluation within a circle of 4 mm in diameter (shown in Fig. 9)

Score	0	1	2	3	4
Giant cells (semi-quantitative)	0–20	21–80	81–140	141–200	>200
Vessels (semi-quantitative)	>150	101–150	51–100	11–50	0–10
Bone reaction (qualitative)	Similar to original cancellous bone	Bone with bone forming activity	Bone with bone forming and osteoclastic activity	Fibrous tissue	Inflammation/necrosis
Interface (qualitative)	Direct bone to implant contact	Remodeling lacuna with osteoblasts and/or osteoclasts at surface	Localized fibrous tissue (not arranged as a capsule)	Fibrous tissue capsule	Inflammation/necrosis
Interstitium within the implant (qualitative)	Mature bone and differentiation of bone marrow	Bone formation	Fibrous connective tissue (characterized by condensation of collagen fibers)	Fibrous connective tissue (with pronounced cellular and vascular component)	No tissue within the implant

Redmond, USA) and SPSS[®] Version 17.0 (SPSS: An IBM Company, Chicago, USA). At first, the metric data were tested for normal distribution using the Kolmogorov–Smirnov procedure. Normally distributed, independent values within the experimental groups were subjected to an ANOVA with subsequent post hoc tests (Tukey), whereas a comparison between the experimental groups at special points in time was done with student's *t*-tests. Not normally distributed, independent values were analyzed using Kruskal–Wallis one-way analysis of variance and following Mann–Whitney *U* tests. In all analyses the level of significance was considered as $P \leq 0.05$.

3 Results

3.1 Sponges

3.1.1 Main elements on the surface detected by SEM/EDX examination of sponges

In the SEM considerable differences could be seen between the sponges. While the pores of the MgF₂ sponge were clearly visible (Fig. 3a), the CaP sponge offered a relatively level surface with thin fissures (Fig. 3d). For the MgF₂ sponge the EDX analysis showed small quantities of the alloying elements aluminum and calcium in addition to a high amount of magnesium. Fluorine was continuously

detectable with 39 wt % in the dark areas and 6 wt % in the bright areas (Fig. 3b). In case of the CaP sponge the EDX analysis revealed calcium, oxygen and phosphorus as main elements in addition to a small quantity of magnesium (Fig. 3e).

3.1.2 Outer and internal sponge structure revealed by μ -computed tomography

In the cross sectional images of the MgF₂ sponge a coating was not definable neither outside nor in the pores (Fig. 3c), whereas the CaP sponges showed coating fractions on the surface and inside the pores (Fig. 3f). According to the 3D calculation results presented in Table 2 about 11 % of the CaP sponges consisted of this considerably denser coating. The volume of the pure CaP sponges was more than twice as high as the MgF₂ sponge volume while having a very similar density. The surface of the pure CaP sponges also increased to almost double the size due to more than double the number of trabeculae with nearly the same trabecular thickness. Hypodense material amounted to a hundredth of the total sponge volume for the MgF₂ sponges and to a fiftieth for the CaP sponges. It was clearly less dense than the sponge material and was seen mostly in trabecular surface wrinkling and loss of substance (Fig. 3c). In consequence of the pores filled primarily with the calcium-phosphate coating, the air volume and porosity of the CaP sponges accounted for one tenth of the MgF₂ sponges. Thereby the CaP sponge pore size

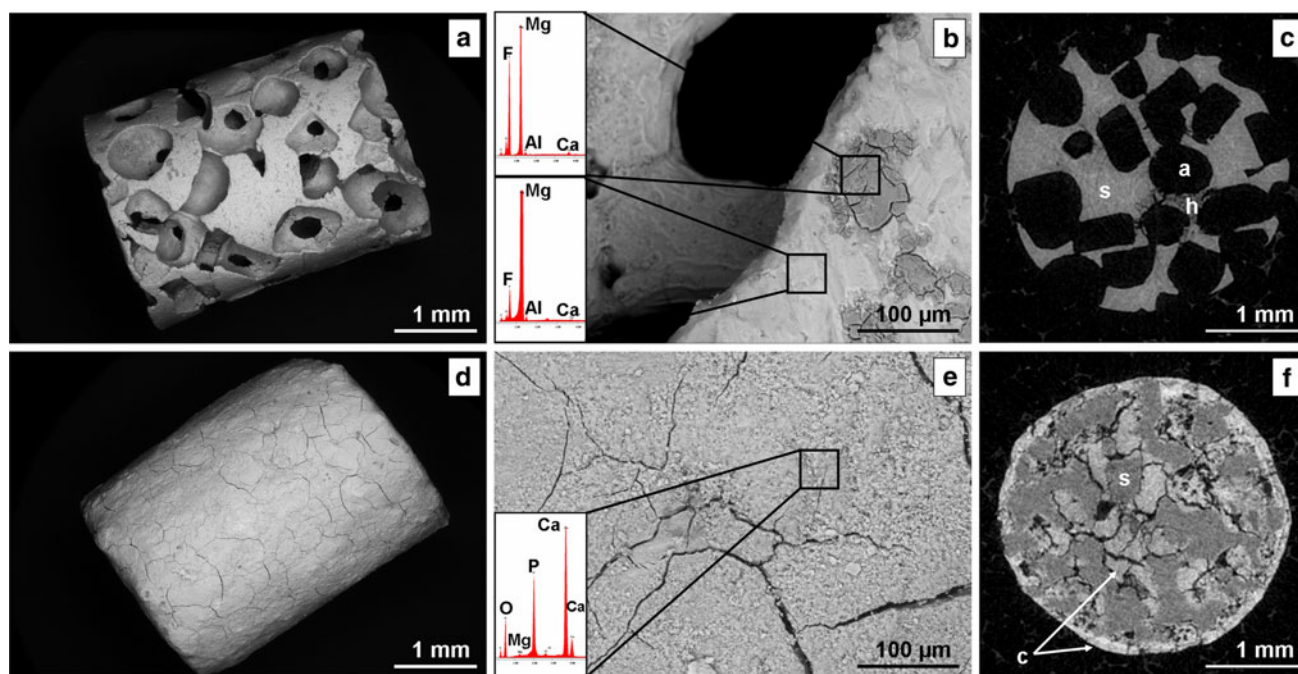


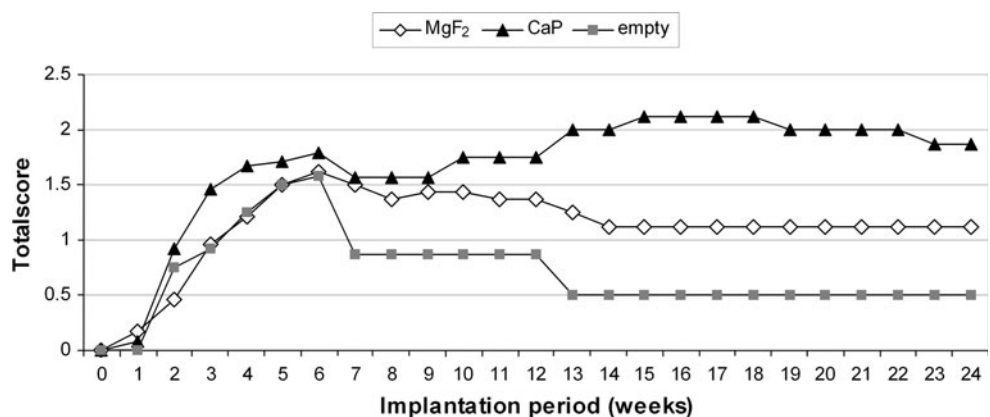
Fig. 3 Pictures of a MgF₂ sponge (on top) and a CaP sponge (at the bottom) before implantation. **a** and **d** SEM pictures of the whole sponge; **b** and **e** magnification and surface EDX analysis in areas

marked with boxes; **c** and **f** μ CT80 cross sections, *c* coating, *s* sponge, *h* hypodense material, *a* air

Table 2 Basic implant properties determined by μ CT80 scan before implantation by using different thresholds for calcium–phosphate coating, magnesium sponge, hypodense material and air; presented as mean and standard deviation

Parameter	(Unit)	MgF ₂ sponges	CaP sponges
Calcium–phosphate coating volume	(mm ³)		2.33 ± 1.88
Calcium–phosphate coating density	(1/cm)		3.07 ± 0.16
Calcium–phosphate coating surface	(mm ²)		108.16 ± 97.62
Magnesium sponge volume	(mm ³)	7.65 ± 1.80	18.35 ± 0.78
Magnesium sponge density	(1/cm)	1.93 ± 0.15	1.86 ± 0.07
Trabecular number	(1/mm)	2.25 ± 0.19	5.10 ± 0.32
Trabecular thickness	(mm)	0.19 ± 0.03	0.18 ± 0.01
Trabecular separation	(mm)	0.49 ± 0.05	0.15 ± 0.02
Magnesium sponge surface	(mm ²)	134.22 ± 15.29	260.61 ± 23.78
Hypodense material volume	(mm ³)	0.07 ± 0.08	0.36 ± 0.31
Hypodense material density	(1/cm)	1.14 ± 0.02	1.12 ± 0.04
Air volume	(mm ³)	14.74 ± 0.93	1.52 ± 0.93
Porosity	(%)	62.73 ± 5.59	5.76 ± 3.75
Pore size	(μ m)	394.40 ± 26.00	109.20 ± 37.30
Variability of pore size	(μ m)	167.30 ± 12.20	72.20 ± 19.60

Fig. 4 Development of the total score values (median) of the HD-radiographs over 24 weeks investigation period. The total score consists of the single score values for periosteal bone formations and bone like structures in the muscle (0 is assessed positive, 2 negative)



represented approximately 28 % of the MgF₂ sponge pore size and showed slightly more differences within the universe, but less variability within a single sponge.

3.2 Postoperative investigation period

3.2.1 Clinical examinations indicated a superior biocompatibility of MgF₂ sponges

Clinically neither pain nor lameness nor wound infections were seen. Postoperative redness, swellings and accumulations of gas receded after 10 days at the latest. Additionally, a clinically apparent, subcutaneous emphysema existed in two cases with CaP sponge from day 14 to 16 and 20, respectively. On average mild peripheral bony augmentations surrounding the drill hole were palpated from 16th to 48th day post operationem in 18/24 limbs with MgF₂ sponge, 17/24 with CaP sponge and 9/12 without implant, whereby the last documented occurrence was at day 98. At the date of euthanasia mild bone

formations were still present in seven cases. In 13 cases with MgF₂ sponge, 18 cases with CaP sponge and 5 cases of the empty group firm structures in the musculature adjoining to the greater trochanter were formed, which were palpable predominantly from day 8 to 15 and up to the end of the experiment.

3.2.2 Radiological examinations revealed minor changes in tissue with implants

In the first postoperative radiographs diffuse gas and gas bubbles were seen in 22/60 cases, evenly distributed over all experimental groups. Only in two cases with CaP sponge the radiographs showed gas bubbles and accordingly diffuse gas in the 2nd week again. Altogether the total score values of all groups (Fig. 4), which depended on bone formations, increased until the 6th week. Especially the periosteal bone formations increased to a higher extent from the 1st week on and reached their highest values with over 6 mm in length and 2 mm in width in all groups

Table 3 Results of the in vivo μ -computed tomographies—score values are given as minimum, median and maximum value for each time period by combining the animal groups at overlapping investigation periods

Test group	Animal group (weeks)	Week	Gas			Bone like structures in adjoining muscle			Periosteal bone formation			Implant integration into bone		
			Min	Med	Max	Min	Med	Max	Min	Med	Max	Min	Med	Max
MgF ₂	6, 12 & 24	0	1	1	2	0	0	0	0	0	0	1	1	1
		2	0	1	2	0	0	2	0	0	1	1	1	1
		4	0	1	1	0	1	2	0	1	2	1	1	2
		6	0	1	1	0	1	2	0	1	2	1	1	2
	12 & 24	8	0	1	1	0	1	2	0	1	2	1	1	2
		12	0	0	1	0	1	2	0	1	1	0	1	2
	24	16	0	0	1	0	1	2	0	1	1	0	0	1
		20	0	0	0	0	1	2	0	1	1	0	0	1
		24	0	0	0	0	1	2	0	1	1	0	0	1
CaP	6, 12 & 24	0	1	2	2	0	0	0	0	0	0	1	1	1
		2	0	0	2	0	0	2	0	0	2	1	1	1
		4	0	0	2	0	1	2	0	1	2	1	1	1
		6	0	0	2	0	1	2	1	1	2	1	1	2
	12 & 24	8	0	0	2	0	1	2	0	1	2	0	1	2
		12	0	0	1	0	1	2	0	1	1	0	1	2
	24	16	0	0	0	0	1.5	2	0	1	1	1	1	2
		20	0	0	0	0	1.5	2	0	1	1	1	1	2
		24	0	0	0	0	1.5	2	0	1	1	0	1	2
Empty	6, 12 & 24	0	1	1	2	0	0	0	0	0	0			
		2	0	0	0	0	0	2	0	0	1			
		4	0	0	0	0	0	0	2	0	1	2		
		6	0	0	0	0	0	0	2	0	1	2		
	12 & 24	8	0	0	0	0	0	1	0	1	2			
		12	0	0	0	0	0	1	0	1	2			
	24	16	0	0	0	0	0	0	0	1	1			
		20	0	0	0	0	0	0	0	1	1			
		24	0	0	0	0	0	0	0	1	1			

0 positive results, 2 negative results

between weeks 4 and 6. The following reduction became most visible in the empty group. The bone-like structures in the adjoining muscle, which were partly found from the 1st week on and never rebuilt, occurred most frequently and in the biggest dimensions by the CaP sponges, what was mainly responsible for the high total score value at the end of the investigation period.

3.2.3 In vivo μ -CT indicated lower gas production and better tolerance of MgF₂ sponges

The first investigations with the XtremeCT showed that all sponges and defects were positioned in cancellous bone. Nearly half of each experimental group reached or broke through the cortical bone, so that a median of 1 was determined in all groups. All other scoring results of the parameters collected regularly within the in vivo μ CT

examination are shown in Table 3. Direct postoperatively gas existed in all cases in varying quantity. Measurable gas bubbles (score 2) from MgF₂ sponges were detected once in week 2, for the CaP sponges five times in week 2 and in single cases up to week 8. In contrast the diffuse occurrence (score 1) was found more often and longer at the MgF₂ sponges. From the 2nd week on no more gas was detectable for the empty drill holes.

The XtremeCT sections showed bony structures with partly trabecular structures in the interior on average from weeks 2 and 4 on and depicted them in the end more often than the radiographs (16 \times MgF₂, 19 \times CaP sponge, 6 \times empty group). In the CaP group the biggest dimensions were determined with sizes up to 4.2 \times 2.5 mm. The decreasing maximum values in the empty group resulted from the fact that the animals with appropriate higher values were randomly distributed to shorter time groups

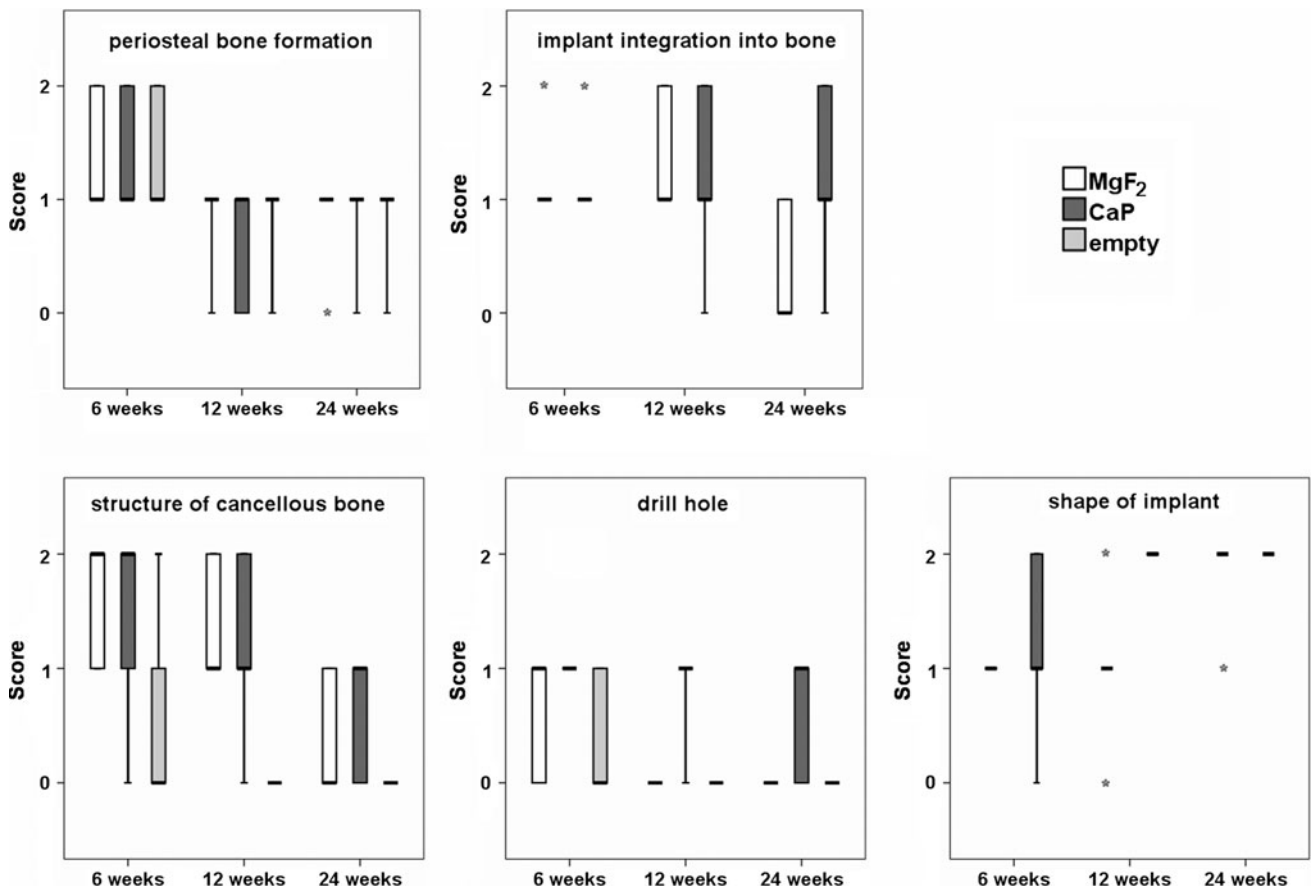


Fig. 5 Ex vivo μ -computed tomographies (μ CT80): Box plots of the greater femur trochanters after 6, 12 and 24 weeks investigation period; thick crossbar median, asterisk outlier (0 describes basic state

and accordingly good integration, 2 was given for clear alterations and accordingly poor integration)

and therefore already euthanized at later times. Regressions were never seen.

According to the radiographs and independent of the experimental group the periosteal bone formations in the drill hole periphery were discernible from the 2nd week on and existed in nearly all cases from the 4th week on. The most bone formations reaching score 2 and thus a size of more than 6×2 mm emerged for the MgF₂ sponges ($n = 4$) in the 4th week, while the peak of the CaP sponges ($n = 8$) and the empty group ($n = 5$) was found in the 6th week. Then they decreased slowly to a score median of 1 with only a few having receded completely until the end of the investigation period.

In the 1st weeks both sponge types showed bone contact at few points. Besides individual poorly integrated sponges this situation persisted for the MgF₂ sponges mainly until week 12, whereas well integrated sponges (score 0) represented the majority from week 16 on. In the CaP sponge groups one very well filled sponge existed at the end of the 12 weeks investigation period and two at the end of a period of 24 weeks. Since on the other hand a lot of CaP sponges lost bone contact completely by a broad gap

formation from week 6 on a generally inhomogeneous integration with little bone contact existed in this group up to week 24.

3.3 Postmortal examinations

3.3.1 Ex vivo μ -CT revealed bone ingrowth and physiological bone healing pattern of MgF₂ sponges despite higher degradation

The scoring results of all evaluated parameters within the μ CT80 are shown in Fig. 5. Regarding the periosteal bone formations and the sponge integration the results of the μ CT80 with a higher resolution corresponded largely to the XtremeCT. But periosteal bone formations, which largest dimension amounted to 10.46×4.17 mm in one slice of a trochanter carrying a CaP sponge, were discernible in all samples even after 6 weeks (Fig. 6d/g).

Bone sponge contact existed for the MgF₂ sponges after 6 weeks primarily in a form of few thin trabeculae extending at and into the outer implant area (Fig. 6a). In addition, after 12 weeks deeper trabeculae ingrowth and isles of bone like

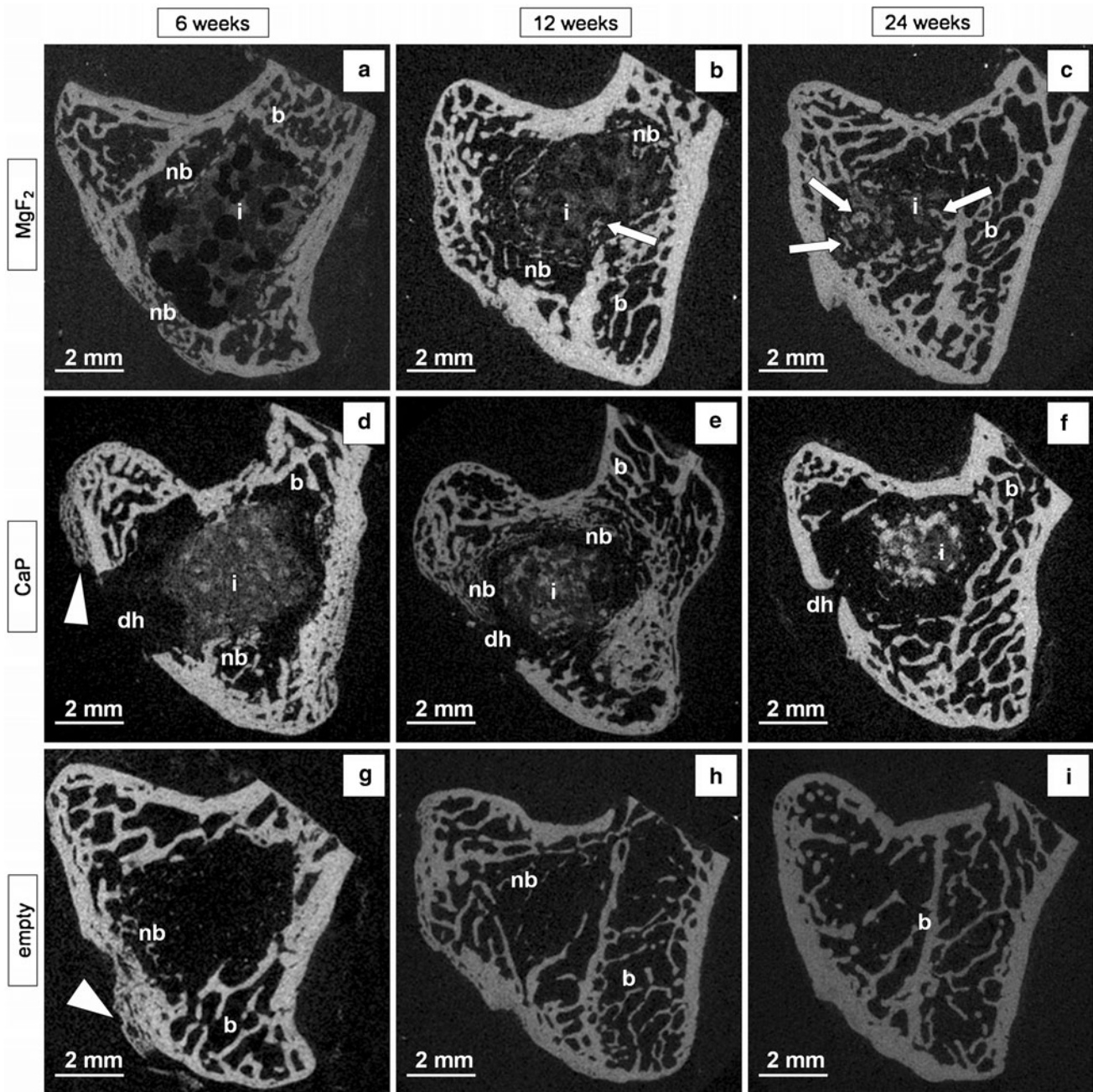


Fig. 6 Ex vivo μ -computed tomographies (μ CT80) after 6, 12 and 24 weeks implantation period. **a–c** bone with MgF_2 sponge (proceeding implant degradation and bone like material in the remaining implant can be seen); **d–f** bone with CaP sponge (merely at the beginning bone trabeculae approach the sponge and the drill hole

material were sporadically observed inside the sponge (Fig. 6b), which increased appreciably after 24 weeks (Fig. 6c). In contrast, for the CaP sponges initially few thick trabeculae grew into the sponge surface cavities, while after 12 and 24 weeks mostly gap formations existed (Fig. 6d, e, f). But in single cases with high sponge degradation also a good filling occurred after 12 and 24 weeks, so altogether the group was very inhomogeneous.

closure is proceeding, but even after 24 weeks incomplete); **g–i** bone with empty drill hole (increasing infiltration of the defect with trabeculae getting thicker from **g** to **i**); **i** implant, **b** bone, **nb** new bone, **dh** drill hole, **arrow** bone like material inside the sponge pores, **triangle** periosteal bone formations

The bone structure differed most notably between the bones with and without implant. Wide-meshed cancellous bone was found in the empty drill holes in almost all cases and especially after 12 and 24 weeks. It filled the defect with fine trabeculae getting thicker in the course of the investigation (Fig. 6g, h, i). After implanting sponges predominantly a development from individual regions of narrow-meshed bone near the sponges after 6 weeks to a

nearly annular occurrence of this structure after 12 weeks and finally to the point of a physiologically wide-meshed bone after 24 weeks was found. However, all MgF₂ sponges exhibited a physiological wide-meshed structure after 24 weeks, whereas CaP sponges still showed both narrow- and wide-meshed bone structure in equal frequencies after 24 weeks.

Regarding the drill hole evaluation the best gap closure existed in the empty group, in which only once an open area remained after 6 weeks. The MgF₂ sponges followed with 5/8 sponges having open drill holes only after 6 weeks. In the CaP sponge group the drill holes were mostly still open at all times. They presented open drill holes at 8/8 after 6 weeks, 6/8 after 12 weeks and 5/8 after

24 weeks. The remaining width of the drill holes is shown in Fig. 7.

The shape of nearly all MgF₂ sponges was still preserved after 6 weeks. However structural changes in the sponge material were recognizable on the basis of different grayscales. After 12 weeks a slightly altered sponge shape manifested and after 24 weeks the shape was clearly changed. In contrast, all CaP sponges except for one showed alterations of shape already after 6 weeks, which increased over time.

All sponge components showed a permanent loss of volume. For the MgF₂ sponges the reduction slowed down continuously and after 24 weeks nearly 24 % of the initial volume still existed on average. For the CaP sponges a relative continuous reduction resulted in approximately 7 % of the initial sponge volume after 24 weeks, while about 17 % of the coating remained after an initially highest, but then clearly decelerating reduction (Table 4).

Also a continuous reduction of the surface existed in all sponge components. However this loss was lower than that of the volume, so that the surface to volume ratio increased. This surface to volume ratio was higher for the MgF₂ sponges at all times, which corresponded with an also optically higher fissuring by a higher number of thinner trabeculae in the course of the degradation. The trabecular number of the CaP sponges did not increase. Regarding the density the MgF₂ sponges showed a significant reduction after 6 weeks and subsequently a slight increase, while that of the CaP sponges and the coating increased slightly consistently.

The bone like fraction within the remaining implant increased continuously for the MgF₂ sponges. A small

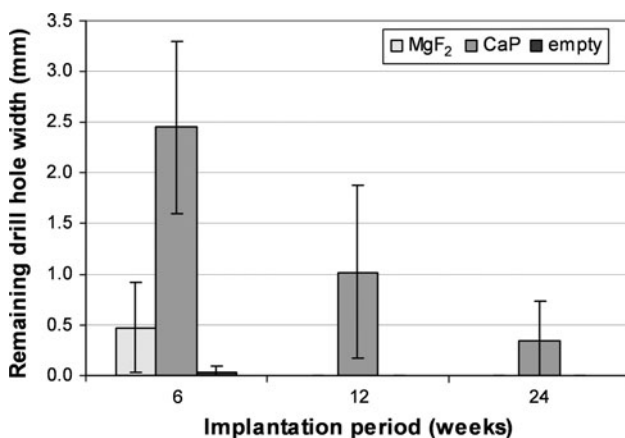


Fig. 7 Development of the drill hole width—measured in the μ CT80 slice with the widest range as distance and presented as mean and standard deviation

Table 4 Development of implant properties and bone like structures in the remaining implant determined in μ CT80 scans with 3D calculations

Parameter (Unit)	Group	0 weeks	6 weeks	12 weeks	24 weeks
Volume (mm ³)	MgF ₂	7.65 ± 1.80 ^a	4.08 ± 1.64 ^a	2.55 ± 2.30	1.83 ± 1.51
	CaPs	18.35 ± 0.78 ^b	7.78 ± 4.98 ^{b, c}	3.39 ± 2.18 ^c	1.31 ± 0.97
	CaPc	2.33 ± 1.88 ^d	0.88 ± 0.93	0.42 ± 0.46 ^d	0.40 ± 0.41
Surface (mm ²)	MgF ₂	134.22 ± 15.29	118.07 ± 30.68 ^e	94.80 ± 43.79	70.74 ± 28.09 ^e
	CaPs	260.61 ± 23.78	217.08 ± 108.05 ^f	108.27 ± 66.19 ^f	48.78 ± 36.13
	CaPc	108.16 ± 97.62 ^g	47.44 ± 45.96	23.13 ± 25.44 ^g	21.70 ± 17.19
Density (1/cm)	MgF ₂	1.93 ± 0.15 ^h	1.76 ± 0.06 ^{h, A}	1.86 ± 0.10	1.85 ± 0.14
	CaPs	1.86 ± 0.07 ⁱ	1.93 ± 0.03 ^A	1.98 ± 0.07 ⁱ	1.98 ± 0.10
	CaPc	3.07 ± 0.16	3.06 ± 0.05	3.18 ± 0.26	3.24 ± 0.12
Bone like fraction inside implant (%)	MgF ₂	0.00 ± 0.00	0.68 ± 0.43 ^B	11.10 ± 8.68 ^j	29.08 ± 13.06 ^{j, C}
	CaPs	0.00 ± 0.00	4.34 ± 1.67 ^B	11.23 ± 18.99	12.18 ± 14.05 ^C
	CaPc	0.00 ± 0.00	4.34 ± 1.67 ^B	11.23 ± 18.99	12.18 ± 14.05 ^C

MgF₂ magnesium sponge inclusive fluoride coating, CaPs magnesium sponge of the CaP sponge, CaPc calcium–phosphate coating of the CaP sponge, surface outer and inner area of the sponges including the pores, bone like fractions tissue inside the sponge with structure and density similar to bone, small letters significant differences within the same group between different time points, capital letters significant differences between different groups at the same time point

Values are given as mean and standard deviation; significances ($P \leq 0.05$)

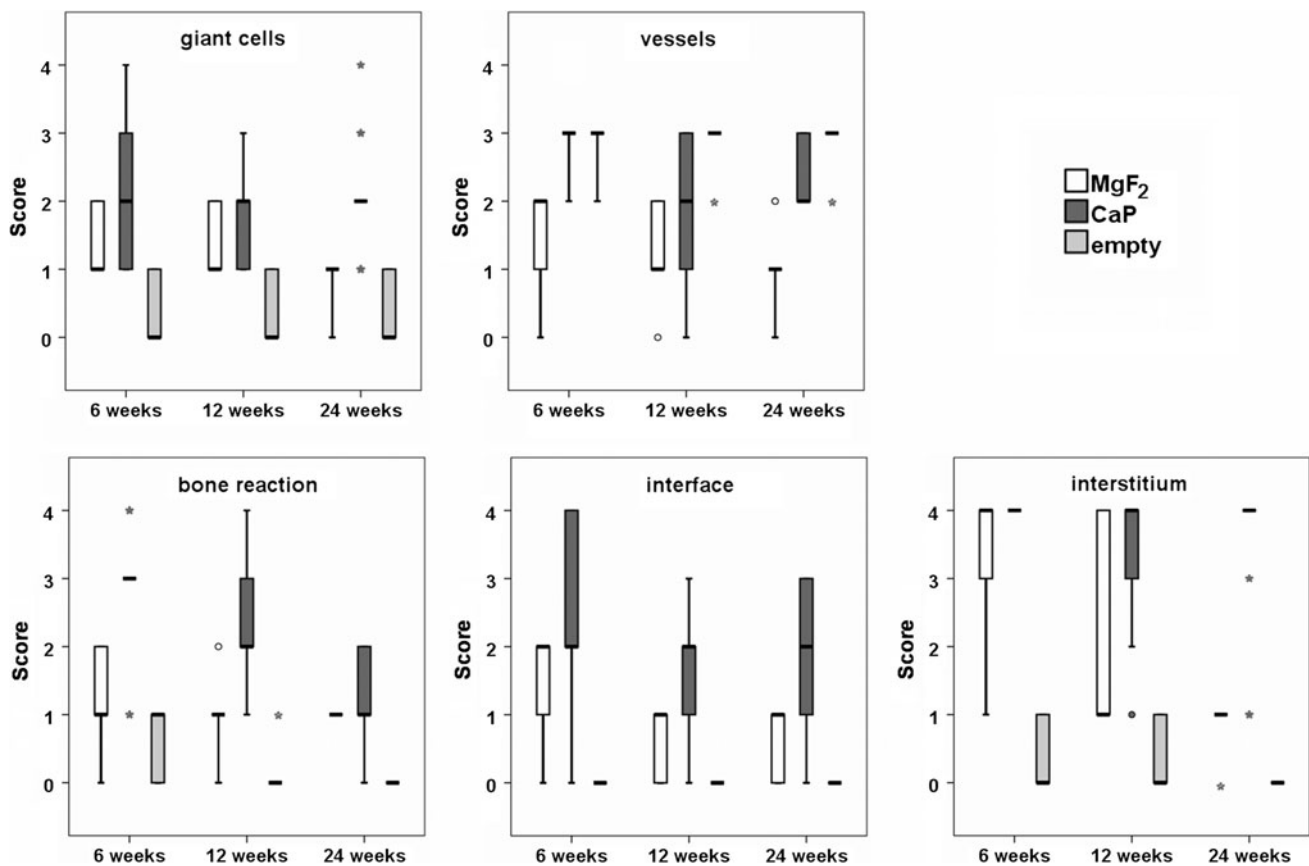


Fig. 8 Histological evaluation: Box plots of the greater femur trochanters after 6, 12 and 24 weeks implantation period; thick crossbar median, circle outliers, asterisk single outlier (corresponding to Table 1 low score values are desirable)

fraction in week 6 was followed by a notably accelerated bone ingrowth, so that a highly significant difference ($P \leq 0.001$) was reached between weeks 12 and 24. In comparison, an obviously higher fraction existed for the CaP sponges after 6 weeks. But since the following increase was less strongly pronounced, the bone like fractions inside both sponge types were similar in week 12 with a clearly higher standard deviation for the CaP sponges. Thereafter a significant difference ($P = 0.026$) could be shown in week 24 due to the distinct increase at the MgF₂ sponges.

3.3.2 Histological analysis showed elevated osteoid production and mildly inflammatory responses of MgF₂ sponges

On average a small amount of foreign body giant cells could be found continually for the MgF₂ sponges during the evaluation according to the scoring system of Table 1. In general more giant cells were found by the CaP sponges and additionally a moderate infiltration with neutrophilic granulocytes after 6 weeks and a mild infiltration with lymphocytes and plasma cells after 12 weeks were noted.

Consistently giant cells rarely existed in the empty drill holes (Fig. 8).

Altogether the highest amounts of vessels were present in the examination area of the MgF₂ sponges. After 6 weeks a lot of capillaries already existed in young fibrous tissue and over 100 were counted on average at later investigation times. The average vascularization rate of the CaP sponges was one level below that of the MgF₂ sponges at each point in time. Merely after 12 weeks single values reached similar levels in both implant groups. With 11–50 on average the fewest vessels were constantly found in the empty group.

A high new bone forming activity in the implant periphery was assessed for the MgF₂ sponges at all three times of investigation (Fig. 9a, b, c). With a high variance the bone reaction of the CaP sponges developed from mainly fibrous tissue formation after 6 weeks to clear bone remodeling with increased osteoclast involvement after 12 weeks and to definite new bone forming activity after 24 weeks (Fig. 9d, e, f). In two CaP sponges of the 6 week group and one of the 24 week group it was not evaluable, because the numerous implant fragments were so widely distributed that only interstitium and interface existed

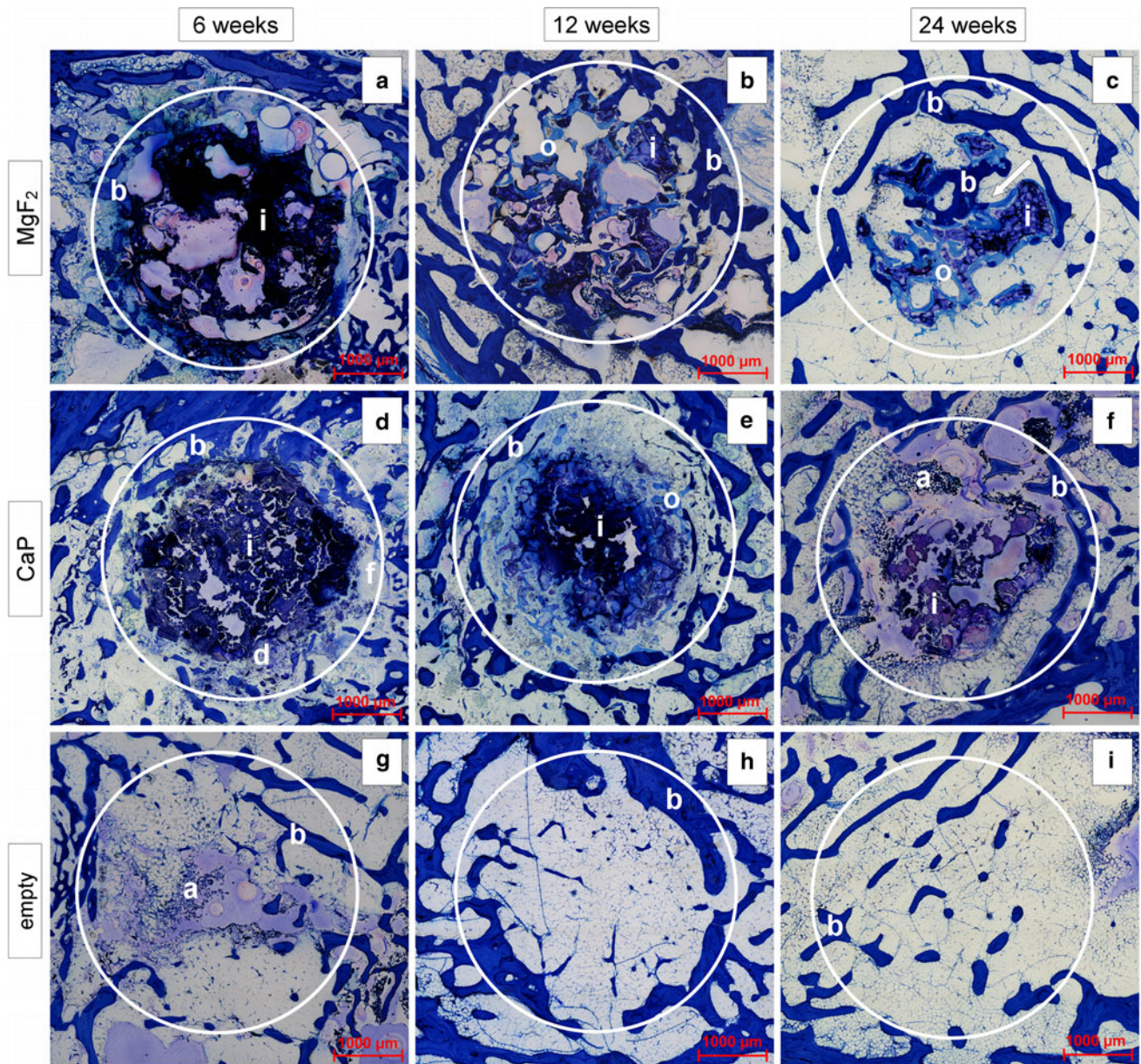


Fig. 9 Photographs of the histological cross sections (*Toluidin blue staining*) after 6, 12 and 24 weeks investigation period. **a–c** MgF₂ sponges in the bone (a clear increase of the osteoid fraction inside the remaining sponge and development of a physiological bone structure); **d–f** CaP sponges in the bone (no bone ingrowth into the sponges, partly distinct osteoid induction, higher levels of debris and

within the examined circle. In the empty group an increased new bone formation activity existed only after 6 weeks. Afterwards the defect periphery was equivalent to physiological cancellous bone (Fig. 9g, h, i).

Osteoid in a small distance from the implant and small areas of fibrous tissue dominated the interface of the MgF₂ sponges after 6 weeks. After 12 and 24 weeks the fibrous tissue was replaced by wide, rarely mineralized osteoid layers and, in single cases, direct sponge bone contact existed. Besides the extraordinary width the osteoid

fibrous tissue in the sponge periphery); **g–i** bone with empty drill hole (increasing infiltration of the defect with bone trabeculae getting gradually thicker, osteoid is hardly present); *circle* region of interest, *i* implant, *b* mineralized bone (dark blue), *o* osteoid (light blue), *d* debris, *f* fibrous tissue, *a* artifacts due to embedding, *arrow* change from osteoid to mineralized bone (Color figure online)

showed typical characteristics like a bone like basic structure and osteoblasts changing into osteocytes inside as well as osteoblasts and lining cells on the surface. The interface of the CaP sponges was dominated continuously by small areas of fibrous tissue, but also fibrous tissue capsules, direct sponge contact and in the 6th week necrosis characterized by cell debris within an amorphous matrix were observed.

Mostly the MgF₂ sponge interstitium contained no tissue after 6 weeks, whereas osteoid has usually grown into the

Table 5 Development of osteoid and mineralized bone fractions in an examined circle area of 4 mm diameter and of the osteoid fraction of the bone matrix—calculated in a histomorphometrical evaluation of Toluidin blue stained cutting and grinding sections

Parameter (unit)	Group	6 weeks	12 weeks	24 weeks
O.Ar/Tt.Ar (%)	MgF ₂	1.75 ± 1.91 ^{a, A, B}	5.53 ± 2.37 ^{C, D}	9.37 ± 3.49 ^{a, F, G}
	CaP	0.09 ± 0.09 ^A	1.77 ± 1.67 ^{C, E}	1.79 ± 1.97 ^{F, H}
	Empty	0.06 ± 0.02 ^{b, B}	0.02 ± 0.01 ^{b, D, E}	0.00 ± 0.01 ^{G, H}
Md.Ar/Tt.Ar (%)	MgF ₂	15.52 ± 6.22 ^I	15.77 ± 5.15	20.42 ± 7.31
	CaP	6.54 ± 3.54 ^I	12.76 ± 10.66	14.43 ± 5.65
	Empty	13.82 ± 6.64	16.21 ± 5.80	16.54 ± 5.38
O.Ar/B.Ar (%)	MgF ₂	8.91 ± 7.65 ^{c, J, K}	25.59 ± 8.73 ^{c, L, M}	31.96 ± 12.16 ^{O, P}
	CaP	1.59 ± 1.87 ^J	10.85 ± 9.41 ^{L, N}	8.80 ± 8.87 ^{O, Q}
	Empty	0.46 ± 0.23 ^{d, K}	0.16 ± 0.12 ^{M, N}	0.02 ± 0.05 ^{d, P, Q}

small letters significant differences within the same group between different time points, *capital letters* significant differences between different groups at the same time point

Values are given as mean and standard deviation; significances ($P \leq 0.05$)

pores after 12 weeks. After 24 weeks the osteoid achieved thicknesses up to 220 µm, revealed mineralizing transition regions (Fig. 9c) and amounted still to the main fraction besides mature bone. Generally the interstitium of the CaP sponges never contained tissue. Only sporadically fibrous connective tissue with pronounced cellular or fiber components or bone formation could be seen. At all times mainly mature bone with wide layers of adipose tissue and zones of hematopoietic tissue existed in the former defect area of the empty group even if the bone trabeculae were very thin after 6 and 12 weeks. The results of the histological scoring are shown in Fig. 8.

Histomorphometrically the O.Ar/Tt.Ar ratio increased perspicuously between weeks 6 and 24 in bones with implant, while it was regressive in bones without implant (Table 5). On the average, it increased the most noticeable for the CaP sponges, but due to inhomogeneity these results were not significant ($P = 0.081$). In contrast, a highly significant difference ($P \leq 0.001$) existed for the MgF₂ sponges between week 6 and 24. The Md.Ar/Tt.Ar ratio increased in all groups over the course of time. In comparison to the control group (16.5 %) it revealed higher values for the MgF₂ sponges (20.4 %) and lower values for the CaP sponges (14.4 %) after 24 weeks investigation period. At all investigation points MgF₂ sponges showed the highest values of O.Ar/B.Ar ratio, which increased significantly ($P = 0.007$) from week 6 to 12. The control group showed the lowest ratio at all times with a significant decrease ($P = 0.007$) from week 6 to 24.

In the examined muscles areas of bone and cartilage tissue were discernible in different sizes, equally distributed over all time and experimental groups. They were located inside mature fibrous tissue fragments, representing scar tissue, with few suture rests and giant cell accumulations.

4 Discussion

The aim of the current study was, firstly, to investigate the biocompatibility, the influence of the surrounding tissue on the ingrowth behavior as well as the degradation of two AX30 sponges possessing different coatings. Secondly, the aim was to determine suitability of these sponges as a synthetic bone replacement material. To avoid excessive corrosion, all sponges were coated with fluoride and half of the coated sponges were additionally provided with a coating containing calcium–phosphate. Following their precise characterization, the sponges were implanted into the cancellous part of rabbit's femur trochanter. In comparison to a control group having empty drill holes, the effects of the sponges were clinically, radiologically and in vivo µ-computed tomographically investigated over time periods of 6, 12 and 24 weeks. On completion of the investigated time period, the sponge carrying bone was additionally investigated by means of high resolution µCT. Finally, these specimen and the adjacent muscles underwent histological examinations.

4.1 Characterization of the biocompatibility of fluoride and calcium–phosphate coated AX30 sponges

In the clinical investigations, it was possible to confirm the good clinical tolerance shown in earlier in vivo studies of magnesium implants [28, 32, 47, 48], also in conjunction with the two sponge coatings employed.

To assess the biocompatibility using the µCT, standardized parameters are used such as the bone implant contact and the fraction of new bone on the implant or defects [1, 2, 26, 49]. Using the in vivo µCT in the current study, it was possible to observe low contact for both types of sponge within the initial weeks, which significantly

increased for the MgF_2 sponge during the course of the investigation period. Corresponding to this, computations on the sponge residue using the high resolution μCT80 demonstrated highly significant increases of the bone like fraction for the MgF_2 sponges. In contrast to the observations using the XtremeCT, a significantly larger fraction was computed for the CaP sponges with the aid of the μCT80 after 6 weeks. However, somewhat larger isolated sponge regions arose by means of crumbling material and new “pores” emerged, which possibly included original bone, which could have lead to erroneously high values. In general, the bone like fraction computations, using the μCT80 evaluations, quantified and confirmed the MgF_2 sponges’ better integration and the overall impression of the *in vivo* μCT evaluation determined per score. The integration behavior of both types of sponge resembled the bioglass coated sponges at early periods during the investigations of Lalk et al. [34]. However, the behavior was clearly better for the MgF_2 sponges during the course of the investigation.

On examining the trabecula’s structure using the μCT80 , one notices that the trabecula, which has grown into the MgF_2 sponge but rarely bonded directly to the implant, appears somewhat thin after 6 and 12 weeks. In addition to this, islands of dense bone, which have no contact with the external bone, existed within the sponge’s interior after 12 and 24 weeks. This could be due to the possibly interjacent located osteoid which was hardly mineralized [38] and therefore did not appear bone-dense in the μCT80 . For the CaP sponges, the physiologically thicker trabecula, which is described in various studies, developed and adjoined directly onto the implant [26, 39, 49]. However, similar to the bare Mg rod samples of Jo et al. [26] and the monolithic sand-blasted MgCa0.8 implants of von der Höh et al. [49], gaps subsequently formed in most, but not in all cases.

On assessing the structure of the surrounding cancellous bone in the presence of a sponge using the μCT80 , narrow-meshed bone developed adjacent to the sponge. This development began in individual regions and then grew into wide-meshed bone via almost annular deposits over a 24 week period. In contrast to the MgF_2 sponges, only half of the CaP sponges reached the final development stages within the 24 weeks. This indicates more rapid bone adaptation to the implant and better tolerance to the MgF_2 sponges. In general, despite the findings in this and the study of Lalk et al. [34], the development of such a structural change does not appear to be necessary since it is not mentioned in numerous other studies [26, 28, 49]. On the other hand, following the implantation of a coated magnesium implant into a rabbit’s femur, Xu et al. also reported a temporary, disorganized and fine-meshed cancellous bone structure and associated this with the stimulation of various growth factors [39].

In comparison to the empty drill holes, reduced bone formation was observed in the μCT80 for trochanters possessing sponges at the cortex of the drilled hole. This reduction in bone formation was significantly more strongly pronounced in the CaP sponges and, in many cases, incomplete even after 24 weeks. According to Henslee et al., these circumstances could be explained by an impediment to the free migration of osteoprogenitor cells due to the scaffold which thereby reduces bone regeneration [2]. For a compacted material such as CaP sponges, this factor would exert a correspondingly stronger influence.

Moreover, all the employed imaging methods depicted the development of periosteal bone formations, which was previously observed by von der Höh et al. [49], in the region of the drill hole. Since the formations also occurred for the empty drill holes, von der Höh et al.’s theory is supported which states that factors independent of the implant; such as drilling into bone, are possible causes for these formations [49]. Despite the fact that the remodeling process, as found by Hampp et al. [41], already began after implantation, no complete remission was verified in the current study.

Histological investigations are essential for further assessing the biocompatibility of a material [45, 50]. It was possible to show in the current study that the MgF_2 sponges activated the most significant bone regeneration and the strongest osteoid production. This resulted in good sponge integration. In contrast to this, only infrequent bone ingrowth, lower vascularization and a higher number of foreign body giant cells and other inflammatory cells were found for the CaP sponges.

Regeneration activity of the cancellous bone was shown in the implant’s surroundings for both the MgF_2 sponges as well as the empty drill holes after 6 weeks. However in contrast to the empty drill holes, this activity continued into the 24th week, which complies with the desired aim of increased bone regeneration by utilizing the implant [2]. Although the CaP sponges also attain the stage of bone regeneration after 24 weeks, as was previously seen in the μCT , they are only enveloped by connective tissue and reactive bone prior to this; as also described for other scaffolds possessing hydroxyl apatite surfaces [1, 30]. Although moderate envelopment with connective tissue can, according to Anderson et al. [51], also be an indication of incipient integration, overall, one must assume a rather worse biocompatibility for the CaP sponges since, in the current study, more frequent connective tissue capsules and zones of necrosis emerged than direct bone contact. Bone growth into the implant only occurred in individual cases. This contrasts with the good filling of the porous implants, made of or possessing materials containing calcium-phosphate, in many other studies [1, 18, 52]. On the other hand however, it also confirms the results of Ekholm et al.

and Fontana et al. [53, 54] who have described an unfavorable or, as the case may be, a non-existent influence of such a coating. The low pore sizes and porosity of, on average, 109 μm and 6 %, respectively, could also provide a possible explanation for the infrequent ingrowth of bone into the CaP sponges. Although pore sizes above 100 μm are considered to be a minimum for cell migration, in many studies, sizes above 300–400 μm turn out to be necessary to regenerate bone and capillaries [55]. Besides this, the porosity for good ingrowth of bone should be as high as possible but may amount to a maximum of 90 % for sufficiently long term strength in degrading implants [55].

In contrast to this, close contact with the new bone, which has previously been described in many magnesium implant studies, mainly develops at the interface region of the MgF_2 sponges due to the formation of unmineralized osteoid [26, 28, 33, 39]. Quantitatively determining the fraction of bone tissue involved in the described bone reaction resulted in a highly significant increase in osteoid ($P \leq 0,001$) between weeks 6 and 24. This osteoid exhibited unusual proportions having a thickness of up to 220 μm . According to Raina [56], osteoid has a maximum thickness of 20 μm during physiological bone regeneration. Since its structure was similar to bone and typical osteoblasts and lining cells on the surface were to be verified in this study, it can nevertheless be assumed that this involves osteoid, defined as non-mineralized bone matrix [46], and not a protein matrix possessing collagen fibrils, such as those which were possible for Gerber et al. [57] to verify on investigating NanoBone[®] in the lower jaw of miniature pigs. The μ -computed tomographic image of very fine and partially non-contiguous trabecula structures also substantiates the intense formation of histologically verifiable, non-mineralized osteoid since non-mineralized bone matrix can not be depicted by means of μ -computed tomographic investigations. A possible explanation for the elevated production of osteoid or the lack of mineralization in such large measures can be sought in the influence of the fluoride. In other in vivo studies, fluoride also leads to the elevated occurrence of osteoid in bone [36–38, 58], whereof the latter explained the higher amount of osteoid in rats with a mitogenic effect of the fluoride on the osteoblasts [58]. Fluoride also caused the production of structurally modified proteoglycans and matrix metalloproteinases which modified the composition of the bone matrix and, possibly, the subsequent mineralization [59, 60].

For the MgF_2 sponges, sponge degradation and bone formation in the form of osteoid adapted to each other to such an extent that it was possible to verify regular bony tissue in the sponge's interior and to attain the desired osseointegration. This represented a significant improvement in comparison to the bioglass coated AX30 sponges of Lalk et al. for which an apparent gap existed between the implant and bone at this point in time [34]. Although the

fractions of osteoid increased for the CaP sponges, this was however significantly lower. Here, it is questionable of whether the effect was caused by fluoride from the inter-layer or by the implant's insertion. This is because the effect was also regularly found to increasing degrees after the bone implant's insertion as documented in the investigations of Guda et al., Witte et al. and Ekholm et al. [1, 33, 53]. In general, further studies must explain whether the osteoid completely mineralizes following the implant's final degradation as can be assumed from the transition zones. It is advantageous that, according to Mousny et al. [38], the initially reduced mineralization rate has no effect on the trabecular and cortical micro hardness values. The highest fraction of osteoid already found in the group having empty drill holes after 6 weeks can be explained by the early defect bridging together with the correspondingly early phase of the highest turnover.

Overall, the fraction of mineralized bone for the MgF_2 sponges was higher than that for the empty drill holes. This might represent a good starting point for the stated objective of achieving nonunion filling by means of the implant. In contrast to this, the CaP sponges consistently exhibit the lowest values and, similar to the implants of Henslee et al. and Ekholm et al. [2, 53], consequently appear to possibly impede the regeneration of bone.

In comparison with the groups, MgF_2 sponges exhibit the highest vascularization. According to Garcia et al. [61], it is not strictly necessary for a bone implant to promote angiogenesis since the intrinsic angiogenic response would activate sufficient vascularization in a nonunion. However, metabolically active osteogenic cells within the implant's interior require a sufficient supply of blood and oxygen for direct osteoneogenesis [50, 55, 62]. Thus, the vascularization for MgF_2 sponges definitely represents an advantage.

The foreign body giant cells, which were semiquantitatively detected and representative of the inflammatory cells, were hardly discernible in the empty drill holes. For the MgF_2 and CaP sponges, these cells were found in mainly small and, on average, in moderate numbers, respectively. Since, as part of the normal wound healing response, the foreign body giant cells are required to remove material which could stimulate the bone to form a thick capsule of connective tissue following the implantation of degradable materials [50], their higher occurrence is not unusual for the trochanters possessing resorbable sponges. On the other hand, a large number of these cells combined with numerous neutrophil granulocytes, lymphocytes and plasma cells and significant formations of connective tissue; such as that observed by Ekholm et al. [53] in both the CaP sponges as well as in hydroxyl apatite coated cellulose sponges, is interpreted as a sign of inferior biocompatibility [50].

The bony structures, which are verifiable in the gluteus superficialis muscle, were the largest in the CaP sponge and

under no circumstances degenerated, and were invariably found in histological association with fiber residues and accumulations of giant cells. Thus, they could be due to chronic irritation or inflammation by the suture material and/or drilling dust since irritation and inflammation activators in animal models are successfully employed to produce heterotopic ossification [63]. Additional calcium–phosphate ceramic particles possibly operate osteo-inductively in the CaP sponges [63].

4.2 Implant degradation behavior of fluoride and calcium–phosphate coated AX30 sponges

In vivo investigations of a bone replacement material's degradation behavior are essential for estimating the time for which the material is available as a key structure for the ingrowth of bone cells [13, 55, 64].

Following 24 weeks, 44 % of the MgF_2 sponge's 6 week volume still existed and 20 % of the CaP sponge's 6 week volume remained. Thus despite significant sponge degradation during the course of the investigation, both new types of coatings lead to a reduced volume loss compared to the bioglass coating used by Lalk et al. [34]: Here, the implants exhibited a residual volume of 13 % for the same time period. In contrast, in a study by Witte et al. [31] AZ91 scaffolds were largely degraded and most of the original magnesium had disappeared after 3 months implantation period in the rabbit femur condyle. The CaP coating's volume loss decelerated so sharply that 95 % of the 12 week volume still remained after 24 weeks. The question remains whether complete decomposition would occur over a longer time period. The surface areas decrease to a lesser extent than the volumes for both types of implant such that the surface to volume ratio increases. This phenomenon presumably provides an increasing number of cells with the possibility of adhering to the surface [65]. However, this is only advantageous without simultaneous surface roughening since it was possible for von der Höh et al. [49] to verify that adhesion worsened in the cancellous bone for magnesium implants possessing rough surfaces. In addition to this, it has to be taken into account that, for the CaP sponges, the computed surfaces of sponge and coating partially lay against each other; thus in some regions, no pores are exhibited and it was therefore not possible for cells to grow into the implant.

Regarding the implant's form and its density, structural changes and diminished density was only noticed during the MgF_2 sponge's investigation after 6 weeks. At later investigation times, shape changes and an increase in density were demonstrated. Thus after 6 weeks, lower density materials such as oxide and hydroxide were presumably included in the computation as already assumed in other studies [32, 66]. This less-dense material alone could

have been subsequently removed or the implant could have decomposed subject to simultaneous deposition of denser calcium–phosphate precipitates containing magnesium. According to Xu et al. [39], such precipitates can arise from magnesium alloys in liquids containing phosphates such as body fluids. For the CaP sponges, density increases and shape changes already occurred from week 6. Here, the decomposition model with precipitate formation just described can be widely assumed owing to the environment which specifically contains phosphate derived from the implant.

The frequently described occurrence of gas during the decomposition of magnesium implants, which is caused by the material's degradation, was, to a very small extent, also discernible in the current study. Therewith, the faster degrading CaP sponges generated a higher amount of gas within the tissue. However, in agreement with other studies [41, 47, 67], the gas occurrence was not clinically relevant, since no animal showed any signs of pain or functional impairment.

An influence of the implant's localization on the implant degradation's overall results is improbable. Although the positions of the implants and the empty drill holes, which were determined directly after surgery using the XtremeCT, varied from completely into almost entirely in the cancellous bone, the distribution was similar for all test groups. In addition to this, in no cases did implants lay in the medullary cavity in which, according to von der Höh et al. [49], other conditions prevail, which significantly influence the implant's degradation.

4.3 Differences in the characterized implant material

In order to gain exact knowledge about the implant material and thereby possible associated differences in the in vivo behavior, the coated sponges were characterized prior to implanting using various investigation methods.

Regarding the sponges' volume and density, the μ -computed tomographic investigations resulted in a considerably higher volume for the CaP sponge possessing a density similar to that for the MgF_2 sponge. Here, it is possible that a part of the coating from the threshold value, optimized for the AX30 sponge, could also have been recorded and included in the sponge computation. The distinguishable and significantly denser part of the coating could have comprised of crystallized material. In the region of the sponge's trabeculae, minimal levels of hypodense material was detected which, for the CaP sponges, was somewhat more strongly pronounced than that for the MgF_2 sponges. This presumably involves corrosion products since the lower density of this material indicates a change in the material's composition [32, 66] and it was frequently impossible to depict various areas of the

trabeculae at these locations. Thus, the additional coating process of the CaP sponges, which exposes the sponges to further liquids, appears to promote somewhat more corrosion than a pure fluoride coating.

Porosity and pore sizes were, on average, 63 % and 394 μm , and 6 % and 109 μm for the MgF_2 and CaP sponges, respectively, so that both types of coating resulted in significantly different implant structures. Kim et al. [68] verified that by repeatedly coating porous ZrO_2 implants using hydroxyl apatite leads to decreasing porosity and pore sizes, and partially obstructed pores. It can be assumed that the elevated number of coating steps in the case of the CaP sponges is likewise responsible for this effect. However, the lower and thereby more precisely adaptable reduction in porosity per step of 4–5 %, which was sought by Kim et al. [68], would also be desirable for the following magnesium sponge coatings. For this purpose, different and especially adapted coating guidelines must be developed owing to magnesium's relatively low melting point (650 °C), compared to that of ZrO_2 (2,680 °C), and its quite high reactivity [69].

The point wise analysis of the respective coating's composition using the SEM with auxiliary EDX resulted in various levels of fluoride contents at different locations of the MgF_2 sponges and thus to successful fluoride deposition on the sponge. Since the original sponge elements; magnesium, aluminum and calcium, were also invariably verifiable, the coating's continuity is, however, not completely ensured. Generally an inhomogeneous fluoride coating could lead to an inhomogeneous degradation behavior and despite the good results presented in this study the continuity of the fluoride coating and consequences should be investigated more specifically especially when bigger implant geometries are examined. Distinct peaks for calcium, phosphorus and oxygen occur for the CaP sponges. This indicates large fractions of calcium–phosphate. The additional elements; magnesium, aluminum and fluorine, which although only verified in very small amounts, could belong to the sponge lying beneath the coating, which could have been detected by means of cracks in the optically very thick coating, or indicate low occurrences of these elements in the coating.

Overall, the characterization showed that significantly different implants are produced from the same initial material by means of the two types of coatings. Moreover, the properties of the original materials also differed to those in other magnesium sponge studies to such an extent that it is not possible to compare the results.

In summarizing, the data indicate that the MgF_2 sponges produce elevated osteoid and bone formations for simultaneously high vascularization, lower inflammation response and good implant filling. Moreover, despite significant implant degradation, the data also suggests good

biocompatibility. In contrast to this, the CaP sponges exhibit a significantly inhomogeneous implant degradation and integration alongside mostly poorer bone forming activity, vascularization and increased inflammation reaction. This indicates an overall poorer biocompatibility although individual, significantly degraded implants were very well filled with mineralized bone. However, to provide a conclusive assessment, further studies of critical size defects are necessary employing, if required, optimized alloys and coatings over longer time periods.

5 Conclusions

Summa summarum the AX30 sponges were clinically tolerated well with both coatings. The present study shows that a fluoride coating could reduce the degradation of AX30 magnesium sponges considerably and cause a good osseointegration by osteoid and mineralized bone. On the other hand the additional calcium–phosphate coating achieved no improvement of the AX30 sponge properties, but resulted in an inhomogeneous degradation with inferior integration into the bone. Summing up the MgF_2 sponges showed a superior biocompatibility and represent a very promising bone replacement material.

Acknowledgments This study is part of the Collaborative Research Centre 599, which is funded by the German Research Foundation (DFG). Special thanks to Melanie Kielhorn, Diana Strauch and Svenja Pfarr for excellent technical support.

References

- Guda T, Walker JA, Pollot BE, Appleford MR, Oh S, Ong JL, Wenke JC. In vivo performance of bilayer hydroxyapatite scaffolds for bone tissue regeneration in the rabbit radius. *J Mater Sci Mater Med*. 2011;22:647–56.
- Henslee AM, Spicer PP, Yoon DM, Nair MB, Meretoja VV, Witherell KE, Jansen JA, Mikos AG, Kasper FK. Biodegradable composite scaffolds incorporating an intramedullary rod and delivering bone morphogenetic protein-2 for stabilization and bone regeneration in segmental long bone defects. *Acta Biomater*. 2011;7:3627–37.
- Kuzyk PRT, Schemitsch EH, Davies JE. A biodegradable scaffold for the treatment of a diaphyseal bone defect of the tibia. *J Orthop Res*. 2010;28:474–80.
- Marti RK, van der Werken C. Autogenous bone grafting in the treatment of nonunions. In: Marti R, Kloen P, editors. Concepts and cases in nonunion treatment. Stuttgart: Thieme; 2011. p. 106–15.
- Gugala Z, Lindsey R, Goglewski S. New approaches in the treatment of critical-size segmental defects in long bones. *Macromol Symp*. 2007;253:147–61.
- Pape HC, Evans A, Kobbe P. Autologous bone graft: properties and techniques. *J Orthop Trauma*. 2010;24:S36–40.
- Donegan DJ, Scolaro J, Matuszewski PE, Mehta S. Staged bone grafting following placement of an antibiotic spacer block for the management of segmental long bone defects. *Orthopedics*. 2011;34:730–5.

8. Dimitriou R, Jones E, McGonagle D, Giannoudis PV. Bone regeneration: current concepts and future directions. *BMC Med*. 2011;9:66.
9. Karger C, Kishi T, Schneider L, Fitoussi F, Masquelet A. Treatment of posttraumatic bone defects by the induced membrane technique. *Orthop Traumatol Surg Res*. 2012;98:97–102.
10. Dimitriou R, Mataliotakis GI, Angoules AG, Kanakaris NK, Giannoudis PV. Complications following autologous bone graft harvesting from the iliac crest and using the RIA: a systematic review. *Injury*. 2011;42:S3–15.
11. Lasanianos NG, Kanakaris NK, Giannoudis PV. Current management of long bone large segmental defects. *Orthop Trauma*. 2010;24:149–63.
12. Nandi SK, Roy S, Mukherjee P, Kundu B, De DK, Basu D. Orthopaedic applications of bone graft & graft substitutes: a review. *Indian J Med Res*. 2010;132:15–30.
13. Hutmacher DW. Scaffolds in tissue engineering bone and cartilage. *Biomaterials*. 2000;21:2529–43.
14. Wei J, Jia J, Wu F, Wei S, Zhou H, Zhang H, Shin J, Liu C. Hierarchically microporous/macroporous scaffold of magnesium-calcium phosphate for bone tissue regeneration. *Biomaterials*. 2010;31:1260–9.
15. Schneider OD, Mohn D, Fuhrer R, Klein K, Kämpf K, Nuss KMR, Sidler M, Zlinszky K, von Rechenberg B, Stark WJ. Biocompatibility and bone formation of flexible, cotton wool-like plga/calcium phosphate nanocomposites in sheep. *Open Orthop J*. 2011;5:63–71.
16. Reig L, Amigo V, Busquets DJ, Calero JA. Development of porous Ti6Al4V samples by microsphere sintering. *J Mater Process Technol*. 2012;212:3–7.
17. Wegener B, Sievers B, Utzschneider S, Müller P, Jansson V, Rößler S, Nies B, Stephani G, Kieback B, Quadbeck P. Microstructure, cytotoxicity and corrosion of powder-metallurgical iron alloys for biodegradable bone replacement materials. *Mater Sci Eng B*. 2011;176:1789–96.
18. Kim Y-, Anirban JM, Song H-, Seo H-, Lee B-. In vitro and in vivo evaluations of 3D porous TCP-coated and non-coated alumina scaffolds. *J Biomater Appl*. 2011;25:539–58.
19. Nguyen TL, Staiger MP, Dias GJ, Woodfield TBF. A novel manufacturing route for fabrication of topologically-ordered porous magnesium scaffolds. *Adv Eng Mater*. 2011;13:872–81.
20. Singh R, Dahotre NB. Corrosion degradation and prevention by surface modification of biometallic materials. *J Mater Sci Mater Med*. 2007;18:725–51.
21. Schultz P, Vautier D, Atallah I, Gentine A, Debry C. Reconstruction of the anterior mandible using a porous titanium implant: a case report. *Rev Laryngol Otol Rhinol*. 2008;129:201–5.
22. Voggenreiter G, Leiting S, Brauer H, Leiting P, Majetschak M, Bardenheuer M, Obertacke U. Immuno-inflammatory tissue reaction to stainless-steel and titanium plates used for internal fixation of long bones. *Biomaterials*. 2003;24:247–54.
23. Mandalunis P, Ubios A. Experimental renal failure and iron overload: a histomorphometric study in rat tibia. *Toxicol Pathol*. 2005;33:398–403.
24. Bach F, Bormann D, Kucharski R, Meyer-Lindenberg A. Magnesium sponges as a bioabsorbable material—attributes and challenges. *Int J Mat Res*. 2007;98:609–12.
25. Witte F, Abeln I, Switzer E, Kaese V, Meyer-Lindenberg A, Windhagen H. Evaluation of the skin sensitizing potential of biodegradable magnesium alloys. *J Biomed Mater Res A*. 2007;86:1041–7.
26. Jo J, Kang B, Shin K, Kim H, Hahn B, Park D, Koh Y. Hydroxyapatite coating on magnesium with MgF₂ interlayer for enhanced corrosion resistance and biocompatibility. *J Mater Sci Mater Med*. 2011;22:2437–47.
27. Thomann M, Krause C, Angrisani N, Bormann D, Hassel T, Windhagen H, Meyer-Lindenberg A. Influence of a magnesium-fluoride coating of magnesium-based implants (MgCa0.8) on degradation in a rabbit model. *J Biomed Mater Res A*. 2010;93:1609–19.
28. Kraus T, Fischerauer SF, Hänzi AC, Uggowitzer PJ, Löffler JF, Weinberg AM. Magnesium alloys for temporary implants in osteosynthesis: in vivo studies of their degradation and interaction with bone. *Acta Biomater*. 2012;8:1230–8.
29. Reifenrath J, Bormann D, Meyer-Lindenberg A. Magnesium alloys as promising degradable implant materials in orthopaedic research. In: Czerwinski F, editor. Magnesium alloys as promising degradable implant materials in orthopaedic research. Ukraine: InTech Publisher; 2011. p. 93–108.
30. Wang H, Guan S, Wang Y, Liu H, Wang H, Wang L, Ren C, Zhu S, Chen K. In vivo degradation behavior of Ca-deficient hydroxyapatite coated Mg-Zn-Ca alloy for bone implant application. *Colloids Surf B Biointerfaces*. 2011;88:254–9.
31. Witte F, Reifenrath J, Müller PP, Crostack HA, Nellesen J, Bach F, Bormann D, Rudert M. Cartilage repair on magnesium scaffolds used as a subchondral bone replacement. *Materialwiss Werkst*. 2006;37:504–8.
32. Huehnenschulte TA, Angrisani N, Rittershaus D, Bormann D, Windhagen H, Meyer-Lindenberg A. In vivo corrosion of two novel magnesium alloys ZEK100 and AX30 and their mechanical suitability as biodegradable implants. *Materials*. 2011;4:1144–67.
33. Witte F, Fischer J, Nellesen J, Vogt C, Vogt J, Donath T, Beckmann F. In vivo corrosion and corrosion protection of magnesium alloy LAE442. *Acta Biomater*. 2010;6:1792–9.
34. Lalk M, Reifenrath J, Rittershaus D, Bormann D, Meyer-Lindenberg A. Biocompatibility and degradation behaviour of degradable magnesium sponges coated with bioglass—method establishment within the framework of a pilot study. *Materialwiss Werkst*. 2010;41:1025–34.
35. Chiu K, Wong M, Cheng F, Man H. Characterization and corrosion studies of fluoride conversion coating on degradable Mg implants. *Surf Coat Technol*. 2007;202:590–8.
36. Susheela AK, Jha M. Cellular and histochemical characteristics of osteoid formed in experimental fluoride poisoning. *Toxicol Lett*. 1983;16:35–40.
37. McCormack AP, Anderson PA, Tencer AF. Effect of controlled local release of sodium fluoride on bone formation: filling a defect in the proximal femoral cortex. *J Orthop Res*. 1993;11:548–55.
38. Mousny M, Omelon S, Wise L, Everett ET, Dumitriu M, Holmyard DP, Banse X, Devogelaer JP, Grynypas MD. Fluoride effects on bone formation and mineralization are influenced by genetics. *Bone*. 2008;43:1067–74.
39. Xu L, Pan F, Yu G, Yang L, Zhang E, Yang K. In vitro and in vivo evaluation of the surface bioactivity of a calcium phosphate coated magnesium alloy. *Biomaterials*. 2009;30:1512–23.
40. Seitz J, Collier K, Wulf E, Bormann D, Bach F. Comparison of the corrosion behavior of coated and uncoated magnesium alloys in an in vitro corrosion environment. *Adv Eng Mater*. 2011;13:B313–23.
41. Hampf C, Ullmann B, Reifenrath J, Angrisani N, Dziuba D, Bormann D, Seitz J, Meyer-Lindenberg A. Research on the biocompatibility of the new magnesium alloy LANd442—an in vivo study in the rabbit tibia over 26 weeks. *Adv Eng Mater*. 2012;14:B28–37.
42. Donath K, Breuner G. A method for the study of undecalcified bones and teeth with attached soft tissues. *J Oral Pathol*. 1982;11:318–26.
43. Huehnenschulte TA, Reifenrath J, von Rechenberg B, Dziuba D, Seitz JM, Bormann D, Windhagen H, Meyer-Lindenberg A. In vivo assessment of the host reactions to the biodegradation of

- the two novel magnesium alloys ZEK100 and AX30 in an animal model. *Biomed Eng Online*. 2012;11:14–42.
44. Janning C, Willbold E, Vogt C, Nellesen J, Meyer-Lindenberg A, Windhagen H, Thorey F, Witte F. Magnesium hydroxide temporarily enhancing osteoblast activity and decreasing the osteoclast number in peri-implant bone remodeling. *Acta Biomater*. 2010;6:1861–8.
 45. Jansen JA, Dhert WJ, van der Waerden JP, von Recum AF. Semi-quantitative and qualitative histologic analysis method for the evaluation of implant biocompatibility. *J Invest Surg*. 1994;7:123–34.
 46. Parfitt AM, Drezner MK, Glorieux FH, Kanis JA, Malluche H, Meunier PJ, Ott SM, Recker RR. Bone histomorphometry: standardization of nomenclature, symbols, and units. Report of the ASBMR Histomorphometry Nomenclature Committee. *J Bone Miner Res*. 1987;2:595–610.
 47. Erdmann N, Angrisani N, Reifenrath J, Lucas A, Thorey F, Bormann D, Meyer-Lindenberg A. Biomechanical testing and degradation analysis of MgCa0.8 alloy screws: a comparative in vivo study in rabbits. *Acta Biomater*. 2011;7:1421–8.
 48. Remennik S, Bartsch I, Willbold E, Witte F, Shechtman D. New, fast corroding high ductility Mg–Bi–Ca and Mg–Bi–Si alloys, with no clinically observable gas formation in bone implants. *Mater Sci Eng B*. 2011;176:1653–9.
 49. von der Höh N, Bormann D, Lucas A, Denkena B, Hackenbroich C, Meyer-Lindenberg A. Influence of different surface machining treatments of magnesium-based resorbable implants on the degradation behavior in rabbits. *Adv Eng Mater*. 2009;11:B47–54.
 50. Nuss KMR, von Rechenberg B. Biocompatibility issues with modern implants in bone—A review for clinical orthopedics. *Open Orthop J*. 2008;2:66–78.
 51. Anderson JM, Rodriguez A, Chang DT. Foreign body reaction to biomaterials. *Semin Immunol*. 2007;20:86–100.
 52. Kon E, Filardo G, Delcogliano M, Fini M, Salamanna F, Giavaresi G, Martin I, Marcacci M. Platelet autologous growth factors decrease the osteochondral regeneration capability of a collagen-hydroxyapatite scaffold in a sheep model. *BMC Musculoskelet Disord*. 2010;11:220.
 53. Ekholm E, Tommila M, Forsback A, Märtson M, Holmbom J, Aäritalo V, Finnberg C, Kuusilehto A, Salonen J, Yli-Urpo A, Penttinen R. Hydroxyapatite coating of cellulose sponge does not improve its osteogenic potency in rat bone. *Acta Biomater*. 2005;1:535–44.
 54. Fontana F, Rocchietta I, Addis A, Schupbach P, Zanotti G, Simion M. Effects of a calcium phosphate coating on the osseointegration of endosseous implants in a rabbit model. *Clin Oral Implants Res*. 2011;22:760–6.
 55. Karageorgiou V, Kaplan D. Porosity of 3D biomaterial scaffolds and osteogenesis. *Biomaterials*. 2005;26:5474–91.
 56. Raina V. Normal osteoid tissue. *J Clin Pathol*. 1972;25:229–32.
 57. Gerber T, Holzhüter G, Götz W, Bienengraber V, Henkel K, Rumpel E. Nanostructuring of biomaterials—a pathway to bone grafting substitute. *Eur J Trauma*. 2006;32:132–40.
 58. Chavassieux P, Boivin G, Serre CM, Meunier PJ. Fluoride increases rat osteoblast function and population after in vivo administration but not after in vitro exposure. *Bone*. 1993;14:721–5.
 59. Waddington RJ, Langley MS. Structural analysis of proteoglycans synthesized by mineralizing bone cells in vitro in the presence of fluoride. *Matrix Biol*. 1998;17:255–68.
 60. Waddington RJ, Langley MS. Altered expression of matrix metalloproteinases within mineralizing bone cells in vitro in the presence of fluoride. *Connect Tissue Res*. 2003;44:88–95.
 61. Garcia P, Pieruschka A, Klein M, Tami A, Histing T, Holstein JH, Scheuer C, Pohlenmann T, Menger MD. Temporal and spatial vascularization patterns of unions and nonunions: role of vascular endothelial growth factor and bone morphogenetic proteins. *J Bone Joint Surg Am*. 2012;94:49–58.
 62. Kuzyk PR, Schemitsch EH. The basic science of peri-implant bone healing. *Indian J Orthop*. 2011;45:108–15.
 63. Kan L, Kessler JA. Animal models of typical heterotopic ossification. *J Biomed Biotechnol*. 2011;2011:1–8.
 64. Witte F, Fischer J, Nellesen J, Crostack HA, Kaese V, Pisch A, Beckmann F, Windhagen H. In vitro and in vivo corrosion measurements of magnesium alloys. *Biomaterials*. 2006;27:1013–8.
 65. O'Brien FJ, Harley BA, Yannas IV, Gibson LJ. The effect of pore size on cell adhesion in collagen-GAG scaffolds. *Biomaterials*. 2005;26:433–41.
 66. Ullmann B, Reifenrath J, Dziuba D, Seitz J, Bormann D, Meyer-Lindenberg A. In vivo degradation behaviour of the magnesium alloy LANd442 in rabbit tibiae. *Materials*. 2011;4:2197–218.
 67. Witte F, Ulrich H, Rudert M, Willbold E. Biodegradable magnesium scaffolds: part 1: appropriate inflammatory response. *J Biomed Mater Res A*. 2007;81:748–56.
 68. Kim H, Lee S, Bae C, Noh Y, Kim H, Kim H, Ko JS. Porous ZrO₂ bone scaffold coated with hydroxyapatite with fluorapatite intermediate layer. *Biomaterials*. 2003;24:3277–84.
 69. Shadanbaz S, Dias GJ. Calcium phosphate coatings on magnesium alloys for biomedical applications: a review. *Acta Biomater*. 2012;8:20–30.